Electrical and Freeze-Fracture Analysis of the Effects of Ionic Cadmium on Cell Membranes of Human Proximal Tubule Cells

Debra J. Hazen-Martin, John H. Todd, Mary Ann Sens, Wasil Khan, John E. Bylander, Brendan J. Smyth, and Donald A. Sens

Department of Pathology and Laboratory Medicine, Medical University of South Carolina, Charleston, SC 29425 USA

We previously reported that cell cultures of human proximal tubule (HPT) cells respond to ionic cadmium in a manner consistent with well-defined Cd^{2+}-elicited responses reported for *in vivo* systems. However, one unique finding was that the transepithelial electrical resistance and tight junction sealing strands were altered as a result of Cd^{2+} exposure at micromolar concentrations. These alterations are reexamined in detail in the present report to determine whether the Cd^{2+}-induced alterations are specific alterations in the tight junction structure or reflect a general alteration in the cell membrane. Exhaustive analysis of tight junction sealing strands demonstrated no significant alterations due to Cd^{2+} exposure, even at the concentration that elicited a significant reduction in transepithelial resistance. Further analysis of intramembrane particle distribution demonstrated a significant increase in apical intramembrane particles, indicating that Cd^{2+} exposure altered the characteristics of the apical cell membrane. Overall, the results were consistent with evidence of Cd^{2+}-induced alteration in the apical cell membrane of the HPT cell. *Key words:* cadmium, cell culture, cell membrane, electrical resistance, freeze fracture, proximal tubule, tight junction. *Environ Health Perspect* 101:510–516(1993)

We previously reported that cell cultures of human proximal tubule (HPT) cells respond to ionic cadmium in a manner consistent with well-defined Cd^{2+}-elicited responses reported for *in vivo* systems (*1,2*). However, one unique finding not previously noted in *in vivo* studies was that exposure to 0.5 µg/ml of Cd^{2+} reduced transepithelial resistance (R_T) and increased fragmentation of tight junction sealing strands. These findings would be consistent with a disruption of the paracellular transport responsibilities of the proximal tubule cells. However, it was concluded, based on ultrastructural and electrical findings, that the changes in tight junction structure and function were but part of the general damage to the cell membrane elicited by Cd^{2+}.

The finding of altered tight junction structure after exposure to Cd^{2+} has been confirmed recently by investigators using the immortal LLC-PK_1 porcine cell line, which possesses many properties of proximal tubule cells (*3,4*). Prozialeck et al. propose that many of the overt toxic effects of Cd^{2+} *in vivo* appear to be a direct consequence of disrupted junctions between cells in various endothelial and epithelial surfaces (*3,4*); this proposal places greater significance on the findings of junctional disruption by Cd^{2+} *in vitro*. Furthermore, recent studies by Janecki and co-workers using electrical analysis (*5*) have demonstrated that Cd^{2+} also disrupts the tight junctions of Sertoli cell monolayers, although no linkage to the *in vivo* situation was explicitly proposed.

The proposal that Cd^{2+}-elicited disruption of tight junctions is linked to toxicity *in vivo* has motivated us to perform a more thorough examination of the effects of Cd^{2+} on the junctions and cell membranes of cultured HPT cells. The goal of this examination is to determine whether disruptions of tight junctions are but one aspect of overall general damage to the cell membrane or a specific event mediated directly by Cd^{2+} exposure. This paper presents the results of an analysis of the effects of Cd^{2+} exposure on the cell membrane and junctional complex using freeze-fracture methodology. Freeze fracture allows visualization of large surface areas of the cell membrane. This is in contrast to cross-sectional profiles of membranes used in the LLC-PK_1 and Sertoli cell studies that give little information on overall membrane structure and organization. The current freeze-fracture analysis is accompanied by the determination of cell toxicity, Na^+,K^+-ATPase activity, and the ability of the cell to accumulate cAMP through forskolin stimulation.

Materials and Methods

Cell Culture

Stock cultures of HPT cells used in experimental protocols were grown in 75-cm^2 T-flasks as described previously by this laboratory (*6*). Briefly, the growth medium was a serum-free formulation consisting of a 1:1 mixture of Dulbecco's modified Eagle's medium (DME; Gibco, Grand Island, New York) and Ham's F-12 growth medium (Gibco) supplemented with selenium (5 ng/ml), insulin (5 µg/ml), transferrin (5 µg/ml), hydrocortisone (36 ng/ml), triiodothyronine (4 pg/ml), and epidermal growth factor (10 ng/ml). All growth medium supplements were obtained from Collaborative Research (Lexington, Massachusetts). The growth surface was treated with a matrix consisting of bovine type 1 collagen (Collagen Corp., Palo Alto, California) with adsorbed fetal calf serum (Gibco) proteins. For use in experimental protocols, we subcultured the cells at either a 1:2 ratio onto additional tissue culture plasticware or at a 3:1 ratio onto Millicell-HA 30-mm filter inserts (Millipore Corp., Bedford, Massachusetts), allowed them to reach confluency (6–7 days after subculture), and exposed the cultures to identical medium containing the various concentrations of cadmium by adding $CdCl_2$. We fed the cells every 3 days. For the studies reported here, the confluent cells were treated with 0.5, 1.0, and 3.0 µg/ml cadmium, and cell viability, transepithelial electrical resistance, cAMP, Na^+,K^+-ATPase activity, and freeze-fracture morphology were determined at various times of exposure.

The HPT cells used in the present study were isolated from a kidney determined to be inappropriate for transplant procedures. The donor kidney was from a 45-year-old female of Asian descent. We isolated 62 75-cm^2 flasks of primary cells from this kidney (passage 1), having a culture life span of 14 passages at a 1:2 subculture ratio. Cells between passage 5 and 7 were used, and these were noted to retain features expected of cells derived from the proximal tubule (*6–9*).

Cell Viability

The HPT cells were grown to confluency on 12-well plates (4.2 cm^2 per well). We determined cell counts using the nuclear stain DAPI (4′,6-diamino-2-phenylindole) and an automatic counting program executed on a Zeiss IBAS 2000 image analysis computer (*10*). After exposing the confluent cells to $CdCl_2$ at a given concentration (0.05, 0.10, 0.5, 1.0, 3.0, 5.0, 7.0 µg/ml) for a given time (1,4,7,10,13 and 16 days), we rinsed the wells containing the monolayers with phosphate-buffered saline, fixed them for 15 min in 70% ethanol, rehydrated the monolayers with phosphate-buffered saline, and stained them with 50 µl of DAPI (10 µg/ml in distilled water). The well was examined under fluorescent illumination at 320× magnification on the Zeiss IM35, an inverted fluorescent microscope linked to the Zeiss IBAS 2000

Address correspondence to D.A. Sens, Department of Pathology and Laboratory Medicine, Medical University of South Carolina, 171 Ashley Avenue, Charleston, SC 29425 USA.

This research was supported by grant ES 04413 from the National Institutes of Health, National Institutes of Environmental Health Sciences. We acknowledge the excellent editorial assistance of Linda McCarson.

Received 12 February 1993; accepted 13 August 1993.

image processor, revealing fluorescent nuclei, which could readily be quantified using an automatic counting program. For each concentration and time point, we determined a minimum of 20 fields per well and 3 wells per data point. Both nuclear counts and total nuclear area were obtained from the program and yielded equivalent results. Viability was expressed as a percentage of control value for cells unexposed to $CdCl_2$.

Transepithelial Resistance

Confluent cultures of cells were subcultured onto matrix-coated Millicell HA tissue culture inserts and fed fresh growth medium every 3 days. After confluency (3 days), the cells were exposed to 0.5, 1.0, 3.0, and 5.0 μg/ml of $CdCl_2$ (apically and basolaterally, apically only, and basolaterally only) and used for determining transepithelial resistance after 4 days of exposure. Both the apical and basolateral compartments of the inserts contained 2.0 ml of growth medium. We placed the cell monolayers into Ussing chambers (MRA Corporation, Clearwater, Florida) and bathed the monolayers with a modified Krebs-Henseleit solution aerated with 5% CO_2 in air. The initial pH of the solution was adjusted with HCl to 7.0, and the temperature was maintained at 37°C. We used a vapor-pressure osmometer to determine the osmolality of the solution (295–300 mosM). The transepithelial specific resistance (R_T) was determined by clamping the monolayer at a hyperpolarizing voltage of 1 mV for approximately 1 sec and observing the resulting transepithelial current. A validating condition for this method of calculating the resistance is that the monolayer displays the characteristics of an ohmic (linear) resistor. The current–voltage relationship was assessed using voltages (+ and -) from 0.5 to 12 mV and a linear current-voltage relationship was obtained. The specific resistance of collagen-coated blank filters was determined to be 3.0 ± 0.5 Ω x cm^2 (n = 5). We did not subtract this value from the resistance values reported for cell monolayers. Data were analyzed with Systat software and when multiple groups were analyzed, the Tukey HSD test was used for comparison between groups when ANOVA revealed differences between groups.

Freeze-Fracture Analysis

Confluent cultures of cells were subcultured onto matrix-coated Millicell HA tissue culture inserts and fed fresh growth medium every 3 days. After confluency (3 days), the cells were exposed to 0.5, 1.0, and 3.0 μg/ml concentrations of $CdCl_2$ and used for freeze-fracture procedures after 4 days of exposure. The detailed freeze fracture procedures used for generating large numbers of fractures of cultured cells have been published previously (*11*). Quantification and analysis of characteristics specific for various aspects of the cell membrane were accomplished using the Zeiss IBAS 2000 image analyzer employing positive prints of freeze-fracture replicas exhibiting flat fracture regions and uniform shadow angles. We used low magnification micrographs (final enlargement 30,000×) for reference purposes and higher magnification micrographs (final enlargement 75,000–125,000×) for quantitative analysis. The number of intramembrane particles (IMPs) found in each membrane domain was determined on the IBAS 2000 using methods outlined by Usui and coworkers (*12*).

For freeze-fracture data analysis, we used the Zeiss IBAS image analysis system in conjunction with Zeiss-Kontron proprietary IBAS 1000 measuring software, a digitizing tablet, and a mouse. This software also performs standard statistical measurements including the mean, standard deviations, and Students' t-tests between two groups. The characteristics of tight junctions were quantified by tracing sealing strand images using the mouse and digitizing tablet and scaling the results to nanometers from a preset magnification factor or measured directly as angles. We measured the particular components of the junctional complexes using the following conventions. The strand length between points of intersection was measured by directly tracing the sealing strand with a mouse from the high magnification electron photomicrograph. The angle of intersection of strands was measured at each intersection, taking only the acute angle using a three-point apex intersection program parameter. In addition, reference cords were drawn perpendicular to the junction (and therefore parallel to the apical to basal axis of the cell). These reference cords were drawn at 0.50-μm intervals such that they were equally spaced across the entire junctional area. Along these reference cords, we counted the number of intersecting strands, producing the mean number of strands. The distance between adjacent strands was measured with a two-point distance program parameter. Finally, we measured the total apical to basal junctional width along the cord using the two-point distance program parameter.

Na^+, K^+-ATPase Determination

Confluent cultures of HPT cells were subcultured onto matrix-coated Millicell HA tissue culture inserts and fed fresh growth medium every 3 days. After confluency (3 days), the cells were exposed to 0.5, 1.0, and 3.0 μg/ml concentrations of $CdCl_2$ and used for determining Na^+,K^+-ATPase after 4 days of exposure.

We determined the activity of Na^+,K^+-ATPase in the HPT cells using the methods of Johnson and co-workers (*13*) and Forbush (*14*). All isolation procedures were performed at 4°C. Seven days after subculture, we rinsed confluent cell monolayers twice with 5 mM Tris-EDTA, pH 7.5. The cells were scraped from the filter inserts and dounce homogenized (15 ml Pyrex Dounce homogenizer, Wheaton Scientific, Millville, New Jersey) using 15 strokes with a loose pestle, followed by 15 strokes with a tight pestle. We clarified the homogenate by centrifugation at 400g for 10 min, collected the supernatant, and centrifuged it at 33,000g for 45 min. The supernatant was discarded, and the resulting pellet was resuspended in 200 μl of homogenizing solution and protein concentration determined.

We determined the enzyme activity by measuring the liberation of inorganic phosphate from ATP. The assay solution consisted of 100 mM NaCl, 3 mM $MgCl_2$, 5 mM NaN_3, 0.5 mM EGTA, 136 mM Tris, and 0.02% deoxycholate, pH 8.0, to which was added either 25 mM KCl or 1 mM ouabain. The enzyme suspension, containing 30–40 μg/ml of protein, was incubated in assay solution in a total volume of 0.4 ml and preincubated for 1 hr at 37°C. The assay was initiated by adding 0.1 ml of Mg-ATP such that the final concentration of ATP was 5 mM. After incubation at 37°C for 30 min, we terminated the reaction by adding 1 ml of solution consisting of ascorbic acid (3.0%), ammonium molybdate (0.5%), sodium dodecyl sulfate (3.0%), and HCl (0.5N) and incubated at 4°C for 10 min. After incubation, 1.5 ml of a solution consisting of sodium citrate (2.0%), sodium arsenite (2.0%), and glacial acetic acid (2.0%) was added and incubated for 10 min at 37°C. The assay tubes were cooled to room temperature and the absorbance determined at 705 nm using a Gilford 250 spectrophotometer. We determined inorganic phosphate (P_i) against standard phosphate solutions. Typically, 6.2 OD units were equal to 1 μmol P_i. Na^+,K^+-ATPase activity was calculated as the difference between P_i liberated in the presence of K^+ and P_i liberated in the presence of ouabain. Na^+,K^+-ATPase activity is expressed as μmol P_i per mg cell protein per hour. Samples were performed in quadruplicate.

Measurement of Adenosine 3′, 5′-monophosphate (cAMP)

Confluent cultures of HPT cells were subcultured onto matrix-coated Millicell HA tissue culture inserts and fed fresh growth

medium every 3 days. After confluency (3 days), the cells were exposed to the three concentrations of $CdCl_2$ and cells were used for determining cAMP after 4 days of exposure.

The determination of cAMP was performed as described previously (*9*), except Millicell inserts were used in place of 24-well culture plates. Briefly, we rinsed cells grown on Millicell inserts and exposed to various $CdCl_2$ concentrations twice with DMEM buffered with 25 mM Hepes and preincubated for the cells for 15 min at room temperature with medium containing the phosphodiesterase inhibitor 3-isobutyl-1-methyl-xanthine (IBMX; 10^{-3} M). The cells were then rinsed and incubated in medium alone or medium containing forskolin (10^{-6} M). We determined cAMP by radioimmunoassay (RIA) using the nonacetylation method of the cyclic AMP [^{125}I] assay system (Amersham, Code 509) and precipitation of the double-antibody complex by centrifugation. Pellets were counted on a Packard Cobra 5010 gamma scintillation counter, and cAMP stimulation was calculated as the ratio of cyclic AMP in cells treated with forskolin to baseline values obtained with cells treated with IBMX alone. Determinations were made in quadruplicate.

Results

HPT Cell Viability

We assessed cell viability to determine the maximum concentrations of Cd^{2+} that the HPT cells could be exposed to without eliciting cell death. This determination was made for two reasons. The techniques we used to determine the effect of Cd^{2+} on tight junction structure and function require conditions in which there cannot be appreciable cell death. Ussing chamber analysis of transport requires a continuous sheet of epithelial cells, adjoined by tight junctions, in order for a transepithelial gradient to be formed. If Cd^{2+} exposure were to result in appreciable cell death, and therefore disruptions in the continuous nature of the monolayer, transepithelial gradients would not be formed. Under these conditions a lack of transepithelial gradients could then be due to a loss of tight junctions or simply a loss of cells. As such, the determination of tight junction structure and function requires a level of Cd^{2+} exposure affecting cell junctions but not cell viability. Furthermore, a level of Cd^{2+} exposure just below that eliciting overt cell death allows the discernment of cell membrane changes while avoiding more general changes normally associated with cell death.

Cell viability was judged over a 16-day period of exposure, and minimal HPT cell death was noted at Cd^{2+} concentrations of 1.0 µg/ml and below (Fig. 1). Increasing the concentration to 3.0 µg/ml resulted in a slight, but insignificant, trend for increased cell death. In contrast, a further increase in Cd^{2+} concentration to either 5.0 or 7.0 µg/ml resulted in significant cell death within 4 days of exposure and greater than 50% cell death by 10 days of exposure. The system used for counting the cells also allows the quantification of mitotic nuclei and the determination of a mitotic index for each concentration and time of exposure. In no instance did the HPT cells undergo appreciable cell division as a result of exposure to Cd^{2+}. Based on these results, R_T, freeze-fracture morphology, cAMP, and Na^+,K^+-ATPase were determined after 4 days of exposure to 0.5, 1.0, and 3.0 µg/ml of Cd^{2+}. These were concentrations and a time of exposure at which Cd^{2+} did not cause overt cell death.

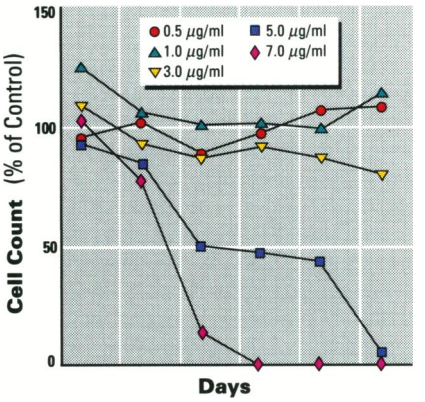

Figure 1. The effect of various concentrations of Cd^{2+}. Results are expressed as the percentage of control values at time points ranging from 1 to 16 days.

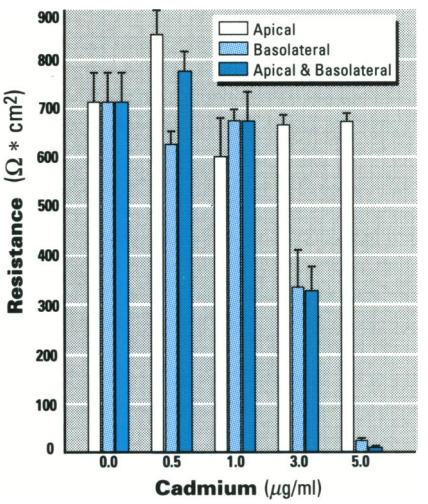

Figure 2. The effect of apical, basolateral, and simultaneous apical and basolateral Cd^{2+} exposure on the transepithelial resistance generated by proximal tubule monolayers.

Transepithelial Resistance

We used classical Ussing chamber analysis to determine the effect of Cd^{2+} on the R_T of the HPT cell monolayers. Exposure of the HPT cells both apically and basolaterally to either 0.5 or 1.0 µg/ml of Cd^{2+} for 4 days had no significant effect on the R_T of HPT cells when compared to unexposed controls (Fig. 2). In contrast, exposure to 3.0 µg/ml of Cd^{2+} for 4 days produced a greater than 50% reduction in the R_T of the HPT cells (Fig. 2). A further increase in Cd^{2+} concentration to 5.0 µg/ml elicited a reduction of R_T to a background level (blank filter). Selective apical exposure of the HPT cells to Cd^{2+} for 4 days resulted in no significant decrease in R_T for cells exposed to 0.5, 1.0, 3.0, and 5.0 µg/ml of Cd^{2+} (Fig. 2). Selective basolateral exposure of the HPT cells to Cd^{2+} for 4 days had identical effects on the R_T as simultaneous apical and basolateral exposure (Fig. 2).

Freeze-Fracture Morphology

Junctional profiles including large areas of adjacent apical and basolateral membrane domains were obtained from each dosage group. The fracture techniques used produced replicas in which apical and basolateral P-face domains predominated. A qualitative assessment of the control fracture images revealed tight junction profiles that were generally composed of three sealing strands arranged in a beltlike array perpendicular to the apical to basal axis of the cell. The strands intersected at various points along their length or were joined by shorter interconnecting strands. The complexity of each junctional profile was largely uniform along the total length exposed by the fracture (Fig. 3). Junctional profiles obtained from cells treated with Cd^{2+} revealed many well-formed junctions. Within each Cd^{2+}-treated group there appeared some evidence of modifications in sealing strand numbers and arrangements. In cells treated with 3.0 µg/ml Cd^{2+}, it was possible to observe areas of junction including 6 or more strands (up to 16 strands) adjacent to the single-strand areas. In addition, the intersecting networks of strands appeared to be more widely spaced, incorporating a larger total junctional area (Fig. 3). Occasional profiles of isolated single strands as well as isolated patches of intersecting strands were observed in the basolateral membrane domain (Fig. 3).

To substantiate these qualitative observations, we assessed a number of parameters quantitatively (Table 1). Quantification of strand numbers intersecting reference cords placed at 0.5-µm intervals along the junction profile revealed that control junctions were composed of 3.1 ± 1.1 strands. With increasing doses of Cd^{2+}, there appeared to be a trend toward greater strand numbers. Cells treated with 3.0 µg/ml Cd^{2+} had junctions composed of 4.5

Table 1. Cell junction parameters

Cd^{2+} (μg/ml)	Mean strand no. along cord	No. of strands <2	No. of strands 2–6	No. of strands >6	Distance between strands (nm)	Junctional width (nm)
0	3.1 ± 1.1	2 (2%)	96 (98%)	0	59.5 ± 16	141.4 ± 67
0.5	2.7 ± 1.3	10 (12%)	70 (85%)	2 (3%)	67.7 ± 15	123.5 ± 53
1.0	2.6 ± 1.0	7 (9%)	73 (91%)	0	77.8 ± 23	127.1 ± 71
3.0	4.5 ± 2.7	6 (5%)	88 (75%)	24 (20%)	114.0 ± 48	349.6 ± 189

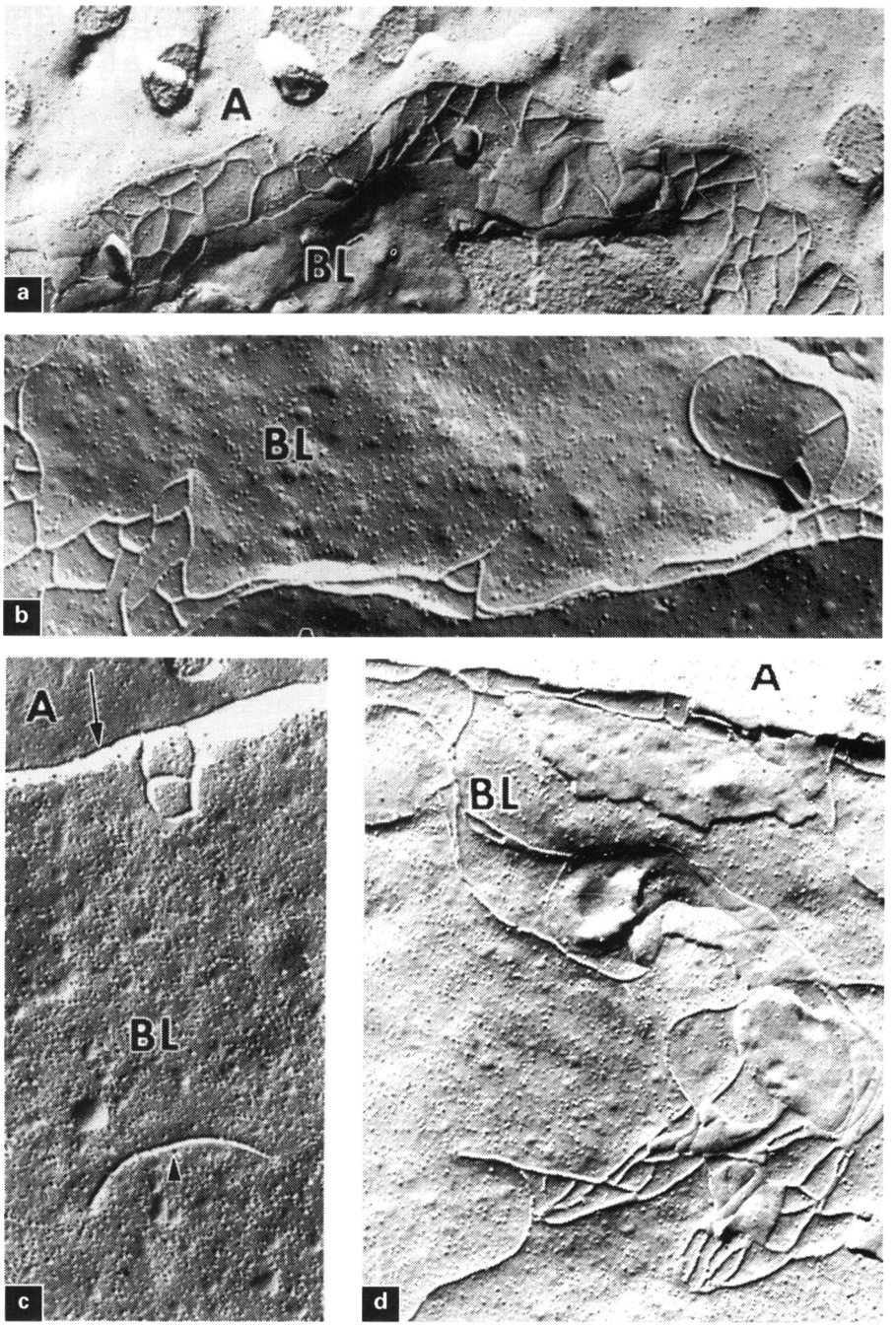

Figure 3. (a) Tight junctions in control cells are composed of several sealing strands along the length of the junction separating the apical (A) and basolateral (BL) domains of the cell membrane (54,000×). (b) Tight junctions in cells exposed to ionic cadmium exhibit arrangements of sealing strands that are less uniform along the length of the junction. The junction appears to involve a greater overall area than those in control cells (54,000×, 3.0 μg/ml Cd^{2+}). (c) Tight junctions in cells exposed to cadmium more frequently included profiles of single-strand junctions (arrow) as well as isolated strands (arrowhead) in the basolateral membrane domain (54,000×, 3.0 μg/ml Cd^{2+}). (d) Complexes of more than six sealing strands were observed in cadmium-treated cells at positions distant from more apically located sealing strands (48,000×, 3.0 μg/ml Cd^{2+}).

± 2.7 strands; however, the standard deviations within each group rendered these differences statistically insignificant. Standard deviations increased with increasing Cd^{2+} dosage. This observation was explained by separating strand counts into three populations (one strand, two to six strands, and greater than six strands). In control cell junctions, 98% of the reference cords intersected between two and six strands, and only 2% intersected a single strand. No profile contained more than six strands along the reference cord.

In contrast, Cd^{2+}-treated junctions included higher percentages of profiles in both the single-strand population and the population including more than six strands, confirming the greater degree of variability along the length of Cd^{2+}-treated junctions. The apical to basolateral distances between strands intersecting a single reference cord were also obtained. Again, a trend toward greater interstrand distances in Cd^{2+}-treated profiles was noted; however, these differences were rendered statistically insignificant due to the large deviations within each group. A measurement of the entire apical to basal junction width also revealed a trend toward greater distances in the Cd^{2+}-treated groups; however, these differences were also insignificant due to the variability within each group. To examine possible differences in junction complexity due to altered patterns of intersection, both the numbers of intersections along lengths of strands and the angles of intersections were quantified (Table 2). Neither parameter was significantly different in any of the experimental groups observed.

Given the variability of strand numbers in different regions along a single-junction profile in Cd^{2+}-treated cells, it was of interest to examine the potential for IMP redistribution between apical and basolateral domains (Table 3). Control replicas revealed a greater concentration of IMPs in the basolateral membrane domain as compared to the apical membrane domain, as is typical of proximal tubule epithelial cells. Similar domains were assessed for IMP density in cells treated with each dose of Cd^{2+}. Particle counts revealed that the application of Cd^{2+} at any dosage did not alter basolateral domain IMP density. However, exposure at the highest tested dosage of Cd^{2+} (3.0 μg/ml) resulted in a significant increase in the number of apical IMPs. This increase was not observed in cells treated with lower dosages of Cd^{2+}. As stated previously, the increase in apical domain IMPs was not accompanied by a corresponding decrease in basolateral IMP numbers, indicating that this change was not a simple redistribution of particles resulting from an alteration in junctional integrity.

Na^+,K^+-ATPase and cAMP

The activity of Na^+,K^+-ATPase was determined on the HPT cells exposed apically and basolaterally to 0.5, 1.0, and 3.0 µg/ml of Cd^{2+} for 4 days. There were no significant Cd^{2+}-induced changes in activity at any of the three concentrations tested (Fig. 4). The ability of the cells to increase cAMP as a result of forskolin treatment was also determined on HPT cells treated as described above. The results demonstrated that Cd^{2+} treatment had no effect on the ability of the cells to respond to forskolin stimulation through an increase in cAMP content (the ratio of unstimulated to stimulated cAMP levels) (Fig. 5).

Discussion

Our initial studies were aimed at determining whether HPT cells could serve as a model for Cd^{2+}-induced nephrotoxicity. These studies (*1,2*) confirmed that Cd^{2+}-initiated changes in human proximal tubule cell cultures mimicked those observed and reported in earlier *in vivo* systems. Furthermore, the *in vitro* model system allowed for more comprehensive studies of functional and structural events without organ or multisystem influences found *in vivo*. These studies showed that decreases in R_T were detectable upon exposure to micromolar concentrations of ionic Cd^{2+}. Caution was used in coupling the resistance data to structural alterations in the tight junction morphology because the alterations were limited to the observation of minimal fragmentation of sealing strands.

Reports by other investigators using LLC-PK1 cells (*3,8*) and Sertoli cells (*5*) demonstrated similar reductions in R_T as a consequence of Cd^{2+} exposure. These findings indicate that the Cd^{2+}-induced reduction in R_T is a repeatable finding, even though the growth media, times, and concentrations of exposure, species, and organ system are different. The tight junction sealing strands are believed to be the structural component underlying R_T. Although previous investigations studied parameters related to junctional integrity such as the cytoskeletal actin arrangement, dome formation, and E-cadherin localization, the analyses of actual changes in tight junction structure proper were limited to the use of routine, thin-section transmission electron microscopy. Such an analysis is limited due to the nature of the thin section specimen. Furthermore, the transmission electron micrographs were derived from cells growing on an impermeable surface, whereas Cd^{2+}-induced alterations in R_T were derived from cultures grown on permeable supports. It is possible that the structural and functional data for a single Cd^{2+} dose cannot be directly coupled when the data are obtained using different growth conditions. The same criticism could be directed at our own early studies, and this resulted in recent advances in this laboratory allowing the visualization of tight junctions by freeze fracture of human proximal tubule cells grown on permeable supports (*11*). Using freeze-fracture analysis of monolayers grown on permeable supports, it is possible to survey a junction along its length and to appreciate the variability that may exist within a single cell. This variability could not be determined by analyzing a single thin section on the identical cell. Our studies indicated that, statistically, there were no differences among control and Cd^{2+}-treated cells in the parameters used to assess junction morphology. The statistical insignificance was due to the variability within the experimental groups. In fact, an increase in standard deviation correlated with increasing Cd^{2+} dosages and was consistent with the qualitative observation that the Cd^{2+}-treated junctions exhibited a less uniform morphology along their length as compared to those of control cells. Overall, the results demonstrated that the Cd^{2+}-induced reduction in R_T was not accompanied by gross alterations in sealing strand structure (i.e., strand fragmentation, disappearance).

One might expect gross alterations in the structure of the sealing strands when R_T is reduced because sealing strand formation has been correlated with the development of R_T (*15*). Furthermore, there is no instance in epithelia where R_T develops in the absence of sealing strand formation. Gross changes in sealing strand structure are absent in these studies, indicating that

Table 2. Intersection parameters

Cd^{2+} (µg/ml)	Total junctional length (µm)	Strand length between Intersections (nm)	Angle of intersection
0	32.36	124.0 ± 66	68.01 ± 7.48
0.5	31.09	149.2 ±108	62.17 ± 9.45
1.0	28.44	166.4 ± 95	66.84 ± 10.14
3.0	34.24	175.5 ± 86	63.43 ± 11.51

Table 3. Intramembrane particle (IMP) distribution

Cd^{2+} (µg/ml)	Face	*N*	IMP/µm² ± SEM
0	Apical P	30	785 ± 66
	Basolateral P	27	1179 ± 46
0.5	Apical P	34	806 ± 44
	Basolateral P	33	1167 ± 23
1.0	Apical P	36	828 ± 33
	Basolateral P	24	1214 ± 31
3.0	Apical P	48	992 ± 35
	Basolateral P	44	1095 ± 34

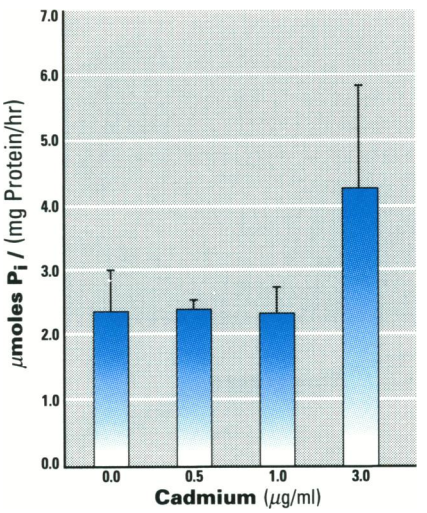

Figure 4. Na^+,K^+-ATPase activity in HPT cells treated with ionic cadmium. Cells growing on Millicell HA filters were exposed to the indicated concentrations of ionic cadmium for 4 days. Values are means ± SE.

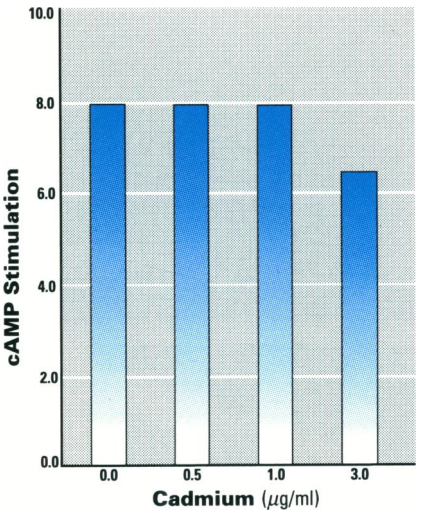

Figure 5. Effect of ionic cadmium treatment on the stimulation of cAMP synthesis in response to 10^{-6} mM forskolin. Cells growing on Millicell filters were exposed to the indicated concentrations of ionic cadmium for 4 days. Values are ratios of the mean cAMP levels ± forskolin.

very subtle changes in morphology of the sealing strands could have significant functional importance in terms of altered R_T. In this regard, the angles of sealing strand intersection were examined in the present study, and these remain unchanged by Cd^{2+} exposure. The sealing strands did exhibit areas of "thinning and thickening" with an overall trend toward increased junctional width due to increased interstrand distances.

Similar observations have been published by other investigators studying alterations in cytosolic Ca^{2+} levels and hydrostatic pressure and their effects on gall bladder epithelium tight junctions (*15,16*). A recent study examining R_T and tight junction morphology as a function of ischemia-induced ATP depletion in MDCK cells adds further evidence that subtle changes in sealing strand morphology can have large effects on R_T (*17*). In these studies, MDCK cells demonstrated an almost total loss of R_T within 10 min of ATP depletion, but with grossly intact sealing strands. Like the present study, no alteration was found in the geometric complexity of the tight junction strands. However, ATP-depleted and control cells did differ in their fracture patterns. Most strands in both ATP-depleted and control cells fractured, leaving ridges on the P-face and complementary furrows on the E-face. However, some of the strands contained sections with a reversed fracture pattern (the P-face ridges contained discontinuities or vacancies, and E-face furrows contained particles). It was shown that these altered patterns were significantly increased in ATP-depleted cells. The authors speculated that these differences could be due to altered patterns of protein phosphorylation (*17*). Together, these studies suggest that subtle alterations in sealing strand morphology can produce large alterations in R_T. Furthermore, these findings indicate that assessing the extent of tight junction structural integrity in pathological situations solely by monitoring transepithelial electrical resistances is not warranted.

The determination of transepithelial electrical resistance provides a measurement of the tight junctions' ability to serve as a gate in regulating the paracellular permeability of ions and macromolecules. An additional function of the tight junction involves its ability to serve as a fence segregating the apical and basolateral membranes into distinct macromolecular domains. One means to determine if the fence function of the tight junction has been compromised is by determining IMP distribution on freeze-fracture replicas. Although the exact composition of IMPs is unknown, they are thought to represent the macromolecular complexes of the cell membrane. For example, there is good evidence that one IMP-associated protein is Na^+,K^+-ATPase (*18*). Na^+,K^+-ATPase is found in both apical and basolateral cell epithelial cell membranes before tight junction formation. Epithelial cells undergo polarization or repolarization by segregation of membrane proteins to specific domains. It is suggested that after tight junction formation, the apically located Na^+,K^+-ATPase is degraded or removed by apical membrane turnover (*18*). As such, if the fence function of the tight junction is compromised, there would be a shift in IMP distribution between the apical and basolateral membrane domains. The current study demonstrated that in no instance did Cd^{2+} exposure result in such a redistribution. This observation demonstrates that Cd^{2+} exposure elicits an alteration in the gate, but not the fence function of the tight junction. Furthermore, the similarity of these findings, with respect to the gate and fence functions, to other renal epithelial cell studies not related to Cd^{2+} exposure indicates that the response may be general in nature. To date, similar results have been found in MDCK cells subjected to ischemia-induced ATP depletion (*17*) and for the currently reported HPT cells when exposed to aminoglycoside antibiotics (*19,20*).

Although no redistribution of IMPs was found as a result of Cd^{2+} exposure, the highest dosage of Cd^{2+} exposure did result in a significant increase in the apical IMP density. This is important information, as a primary goal of this study was to determine whether disruptions of tight junctions are simply one aspect of general damage to the cell membrane or a specific event. The increased density of IMPs in the apical membrane provides a general measure of apical membrane structure and could result from a variety of alterations in membrane trafficking, protein degradation, or disaggregation of apical structures. Furthermore, it has been previously shown in these cells that apical microvilli are altered as a function of Cd^{2+} exposure (*1,2*). This, coupled with the current demonstration of an alteration in apical membrane IMP density and subtle differences in tight junction structure, provides evidence that the alteration in R_T is but one of a spectrum of membrane alterations elicited by Cd^{2+} exposure.

The finding that the reduction in R_T and alterations in membrane structure were mediated through selective basolateral exposure to Cd^{2+} was unexpected. However, basolateral sensitivity has been reported for overt cell toxicity by another research group when cultured LLC-PK_1 cells were exposed to Cd^{2+} (*21*). The findings are surprising because one would expect the added Cd^{2+} to quickly penetrate the cellular junctions and redistribute rapidly to both the apical and basolateral solutions bathing the cell membrane. In fact, it was found in the LLC-PK_1 study (*21*) that Cd^{2+} placed either apically or basolaterally did completely redistribute to the opposite side within 24 hr of exposure. A similar pattern of redistribution was also found for the HPT cells (J.E. Bylander, unpublished observations). It was also demonstrated that the basolaterally located cAMP system was unaffected by Cd^{2+} exposure. One possible explanation underlying these findings is a difference in the induction of the protective protein metallothionein depending on apical or basolateral exposure. If apical exposure is more effective in the induction of metallothionein, the cell would then be expected to be more resistant to the early effects of Cd^{2+} exposure by that route. LLC-PK_1 cells are known to induce metallothionein upon Cd^{2+} exposure (*22*), as are the HPT cells (*23*). The possibility of differences in induction as a result of selective apical or basolateral exposure is under current investigation.

References

1. Hazen-Martin DJ, Sens DA, Blackburn JG, Sens MA. Cadmium nephrotoxicity in human proximal tubule cell cultures. In Vitro Cell Dev Biol 25:784–790(1989).
2. Hazen-Martin DJ, Sens DA, Blackburn JG, Flath MC, Sens MA. An electrophysiological freeze fracture assessment of cadmium nephrotoxicity in vitro. In Vitro Cell Dev Biol 25:791–799(1989).
3. Prozialeck WC, Niewenhuis RJ. Cadmium (Cd^{2+}) disrupts intercellular junctions and actin filaments in LLC-PK_1 cells. Toxicol Appl Pharmacol 107:81–97(1991).
4. Prozialeck WC, Niewenhuis RJ. Cadmium (Cd^{2+}) disrupts Ca^{2+}-dependent cell-cell junctions and alters the pattern of E-cadherin immunofluorescence in LLC-PK_1 cells. Biochem Biophys Res Commun 181:1118–1124(1991).
5. Janecki A, Jakubowjak A, Steinberger A. Effect of cadmium chloride on transepithelial electrical resistance of sertoli cell monolayers in two-compartment cultures—a new model for toxicological investigations of the "blood-testis" barrier in vitro. Toxicol Appl Pharmacol 112:51–57(1992).
6. Detrisac CJ, Sens MA, Garvin AJ, Spicer SS, Sens DA. Tissue culture of human kidney epithelial cells of proximal tubule origin. Kidney Int 25:383–390(1984).
7. Blackburn JG, Hazen-Martin DJ, Detrisac CJ, Sens DA. Electrophysiology and ultrastructure of cultured proximal tubule cells. Kidney Int 33:508–516(1988).
8. Middleton JP, Dunham CB, Onorato JJ, Sens DA, Dennis VW. Protein kinase A, cytosolic calcium and phosphate uptake in human proximal renal cells. Am J Physiol 257: F631–F638(1989).
9. Flath MC, Bylander JE, Sens DA. Variation in sorbitol accumulation and polyol pathway activity in cultured human proximal tubule cells. Diabetes 41:1050–1055(1992).
10. Tarnowski BI, Sens DA, Nicholson JH, Hazen-Martin DJ, Garvin AJ, Sens MA.

Automatic quantitation of cell growth and determination of mitotic index using DAPI nuclear staining. Pediatr Pathol 13:231–244 (1993).
11. Todd JH, Sens DA, Sens MA, Hazen-Martin DJ. In situ freeze-fracture of monolayer cell cultures grown on a permeable support. Micros Res Technol 22:301–305(1992).
12. Usui N, Takahashi I, Koga T, Kawaguchi J. A quantitative study of freeze-fractured biological membranes using an image analyzer. J Electron Microsc 33:363–370(1994).
13. Johnson JP, Jones D, Weismann WP. Hormonal regulation of Na,K-ATPase in cultured epithelial cells. Am J Physiol 251:C186–C190(1986).
14. Forbush B. Assay of Na,K-ATPase in plasma membrane preparations. Increasing the permeability of membrane vesicles using sodium dodecyl sulfate buffered with bovine serum albumin. Anal Biochem 128:159–163(1983).
15. Bentzel CJ, Palant CE, Fromm M. Physiological and Pathological Factors Affecting the Tight Junction. In: Tight junctions (Cereijido M, ed). Boca Raton, FL:CRC Press, 1991; 151–173.
16. Palant CE, Duffy ME, Mookerjee BK, Ho S, Bentzel CJ. Ca^{2+} regulation of tight junction permeability and structure in necturus gallbladder. Am J Physiol. 245:C203–C213 (1983).
17. Mandel LJ, Bacallao R, Zampighi G. Uncoupling of the molecular 'fence' and paracellular 'gate' functions in epithelial tight junctions. Nature 361:552–555(1993).
18. Hammerton RW, Nelson WJ. Mechanisms Involved in spatial localization of Na^+K^+-ATPase in polarized epithelial cells. In: Tight junctions (Cereijido M, ed). Boca Raton, FL: CRC Press, 1991; 215–230.
19. Sens MA, Todd JH, Hazen-Martin DJ, Sens DA. Aminoglycosides disrupt paracellular transport of cultured human proximal tubule (HPT) cells. FASEB J 6:1194A(1992).
20. Todd JH, Sens DA, Hazen-Martin DJ, Sens MA. Aminoglycoside antibiotics alter the paracellular transport properties of cultured human proximal tubule cells. Toxicol Pathol (in press).
21. Bruggeman IM, Temmink JHM, van Bladeren PJ. Effect of glutathione and cysteine on apical and basolateral uptake and toxicity of $CdCl_2$ in kidney cells (LLC-PK_1). Toxicol In Vitro 6:195–200(1992).
22. Felley-Bosco E, Diezi J. Cadmium uptake and induction of metallothionein synthesis in a renal epithelial cell line (LLC-PK_1). Arch Toxicol 65:160–163(1991).
23. Bylander JE, Shuli L, Sens MA, Hazen-Martin DJ, Re GG, Sens DA. Induction of metallothionein mRNA and protein following exposure of cultured human proximal tubule cells to cadmium. Toxicol Lett (in press).